1.Introduction

Bulk Silicon is the indirect band gap material, in which non radiative combination rates are much higher than the radiative recombination rates. This yields to the poor quantum efficiency in the order of 10^{-6} for silicon luminescence. In addition, at the high pumping rates needed to achieve optical amplification fast non radiative processes such as Auger or free carrier absorption severely prevent population inversion. Nano structured silicon overcomes some of these material limiations. Efficient room temperature visible emission can be achieved in various form of nanostructured silicon such as porous silicon, silicon quantum wells, quantum dots or silicon nanocrystals.

Key factors that affect the quantum efficiency of Si nanocrystals are Auger recombination, quantum confined stark effect and coulomb charging of Si nanocrystals.

Microcavities and Quantum confinement effect become prominent in making Si laser possible and feasible[1].

2.NanoStructured Silicon

2.1.Microcavity

When a semiconductor layer is placed in between an optical microcavity, Any slight change in the refractive index will induce a change in the reflectivity spectrum as well as in its photoluminescence spectrum [1]. The porous silicon microcavity was formed with a porous silicon active layer in the middle and sandwiched in between two multi-layered Bragg reflectors. Compared with a porous silicon single layer, the peak value of the emission intensity increased and the full width at half maximum value of the photoluminescence resonance noticeably narrowed when a microcavity structure was used [2]. The luminescence from a microcavity resonator is highly directional, so the power efficiency is improved because the loss of optical power along unwanted directions is minimized [3]. In semiconductor microcavities, the motion of photons and excitons (bound electron-hole pairs) is quantum confined along the growth direction of the semiconductor structure. Indeed, the cavity photons are trapped by dielectric mirrors, while the excitons are confined in quantum wells. The absorption of photons in the quantum well create excitons. The destruction of excitons creates cavity photons. The alternance of the absorption and emission process is nearly reversible (strong exciton-photon coupling). The strong coupling between cavity photons and quantum well excitons gives rise to exotic composite particles, the so-called polaritons. In the moderate density regime, polaritons behave like interacting bosons. The parametric interactions between pair of polaritons are responsible for efficient and ultrafast stimulated amplification [4].

2.2.Porous Silicon

Porous silicon can be made by dissolving a bulk silicon wafer in an electrochemical cell containing hydrogen fluoride solution. The remaining porous layer is a complicated network of silicon wires each with a thickness of between 2-5 nm (20,000 times thinner than a human hair). The porosity of a sample is defined as the amount of air in the material after processing has finished, so a 45% porous sample would contain 45% air and 55% silicon. A typical sample could have an internal surface area of up to several hundred square meters per cubic centimeter.

Light emission from porous silicon occurs mainly in the visible region of the electromagnetic spectrum. The emission has the unique property that the wavelength of the emitted light can be changed simply by increasing or decreasing the porosity of the material. For example, a highly porous sample (70-80% porosity) will emit green/blue light while a less porous sample (40%) will emit red light [5].

2.3.Quantum Dots and Wires

In a quantum wire the electron movement is confined in two out of three directions in space, i.e. it can only move along the wire. To drastically affect the properties of the material the diameter of the wire need to get close to 100 Å. In a quantum dot the electron movement is confined in all three directions. The quantum dot can be looked upon as a man made atom, fabricated out of approximately 1000 real atoms [6].

2.4.Quantum Wells

When an electric field is applied perpendicular to the surface of a quantum well, the optical absorption of the quantum well can be changed. This change in absorption is relatively large. In practice this means we can make small and efficient optical modulators using quantum wells [7].

A QW is a very thin semiconductor layer,typically 10 nm, sandwiched between ‘barriers’ of larger bandgap. Because of the bandgap difference, electrons and holes are trapped in the QW. The small size of the well causes the electron and hole energy levels to become quantized, and so the bandgap energy of a QW is larger than that of an equivalent bulk layer [8].

3.Plasma Enhanced Chemical Vapor Deposition of Silicon Nanocrystals

Substoichiometric SiO_x are deposited on a quartz substrate on a quartz substrate in a three layer waveguide geometry using parallel plate PECVD system followed by high temperature thermal annealing as shown [1].

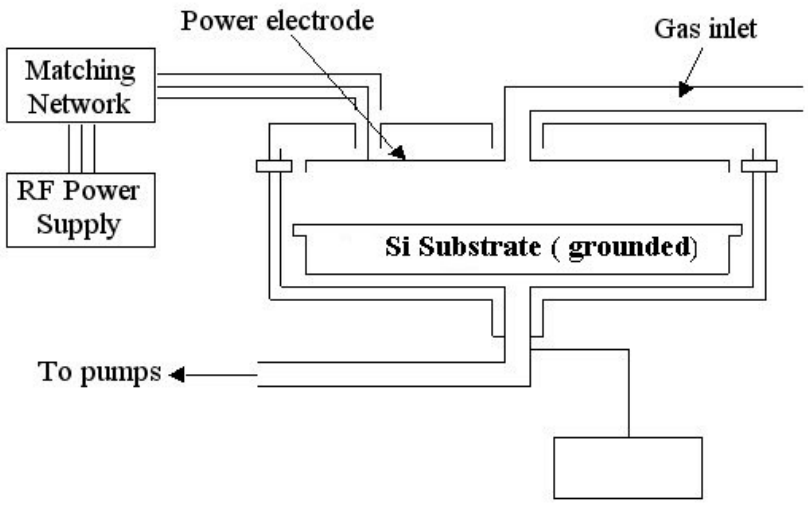

Fig.3.1 Schematic of PECVD System

PECVD system consists of an ultra high vacuum chamber with base pressure 1E-9 Torr and a RF power supply (13.56 MHz) connected through a matching network to the top electrode of the reactor; the bottom electrode is grounded and acts also as the sample holder. Czochralski silicon wafers (5 in diameter, 100 orientation) have been heated at 300 deg C during deposition. The source gases used are high purity (99.99 % or higher) SiH4 and N2O; the N2O/SiH4 flow ratio ã has been varied between 6 and 15, while keeping the total flow rate constant, at a value of about 140 sccm. The total pressure during deposition processes has been maintained constant at a value

of about 6E-2 Torr. After deposition, the SiOx films have been annealed for 1 h at temperatures between 1000 and 1250 °C in ultra pure nitrogen atmosphere using a horizontal furnace [2].

The Overall reaction is as follows:

$SiH_4 + 2\ N_2O \lozenge\ \ SiO_2 + 2\ H_2O + 2\ N_2$

Gas phase decomposition of N2O initiates the reaction. A series of radical chain reactions then leads to the formation of stochiometric oxide when the N2O/SiH4 is about 100. At lower ratios, the reaction of SiH2 with N2O produces silicon rich films with 02 as an additive to control stochiometry[4].

Annealing seperates SiOx into Si nanocrystals (NC) and SiO2.The pictorial representation of the whole process is shown in fig 3.2.

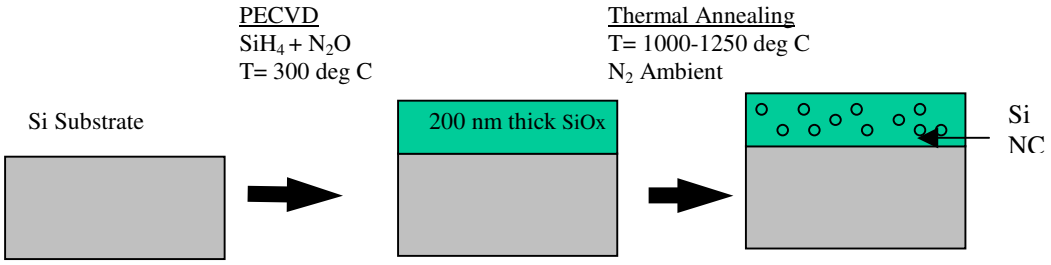

Fig.3.2 Si Nano crystal Formation using PECVD

The composition of samples, as deduced from Rutherford backscattering spectrometry (RBS) measurement, are summarized in table 3.1[2].

		Composition (at. %)		
γ	Sample	Si	O	N
15	S0	33	58	9
10	S1	35	51	14
8	S2	37	51	12
7.5	S3	39	49	12
6.5	S4	42	48	10
6	S5	44	47	9

Table 3.1 (N2O/SiH4 flow ratio is α)

Light emission from as-deposited SiO*x* samples has been found in all cases to consist of weak signals, having a typical wavelength around 600–650 nm. On the other hand, all SiO*x* samples exhibit a strong room-temperature PL (several orders of magnitude higher than the signals coming from the as-deposited samples) in the 650–950 nm range already after annealing at 1000 °C, with the only exception being the sample with the lower Si content (S1), for which 1100 °C is the minimum required temperature to observe light emission. All PL peaks in the annealed samples are Gaussian shaped as shown in fig 3.3.a [2].

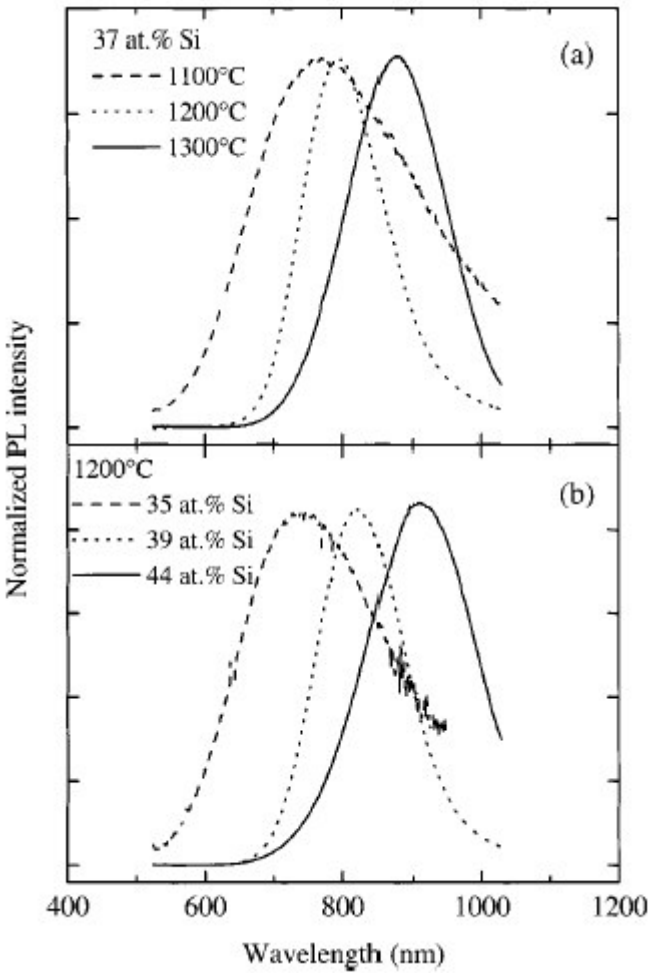

Fig.3.3. Normalized room-temperature PL spectra of **(a)** a SiO film having a Si concentration of 37 at. % (also denoted as S2) after thermal annealing processes performed at 1100, 1200, and 1300 °C for 1 h; **(b)** SiO*x* films having Si concentrations of 35, 39, and 44 at. % (also denoted as S1, S3, and S5) after a thermal annealing process performed at 1200 °C for 1 h.

Fig. 3.3.b shows the PL spectra of three different SiO*x* samples after the same annealing process at 1200 °C. The PL peak is observed at 740 nm for sample S1 (35 at.% Si), at 825 nm for sample S3 (39 at.%Si), and finally at 910 nm for sample S5 (44 at.% Si).The light emission dependence on Si NC mean radius is also shown in fig. 3.4 [3].It is clearly evident that the PL peak is shifted to higher wavelength as the Si NC mean radius increases.

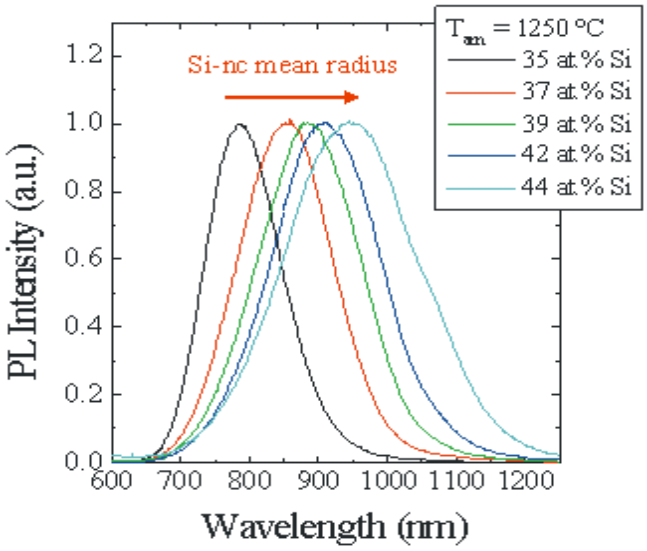

Fig.3.4. PL dependence on mean radius of Si NC

The dependence of PL peaks on both Si NC mean radius and annealing temperature are summarized in Fig.3.5

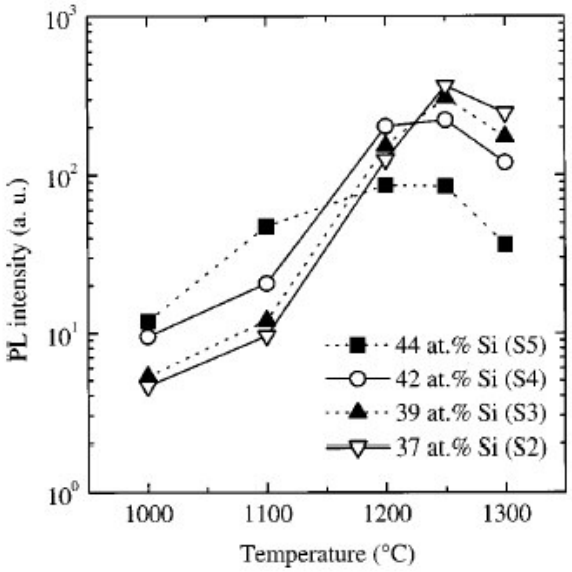

Fig 3.5. Dependence of the integrated intensity of the PL peaks on the annealing temperature for SiO*x* films having different Si concentrations.

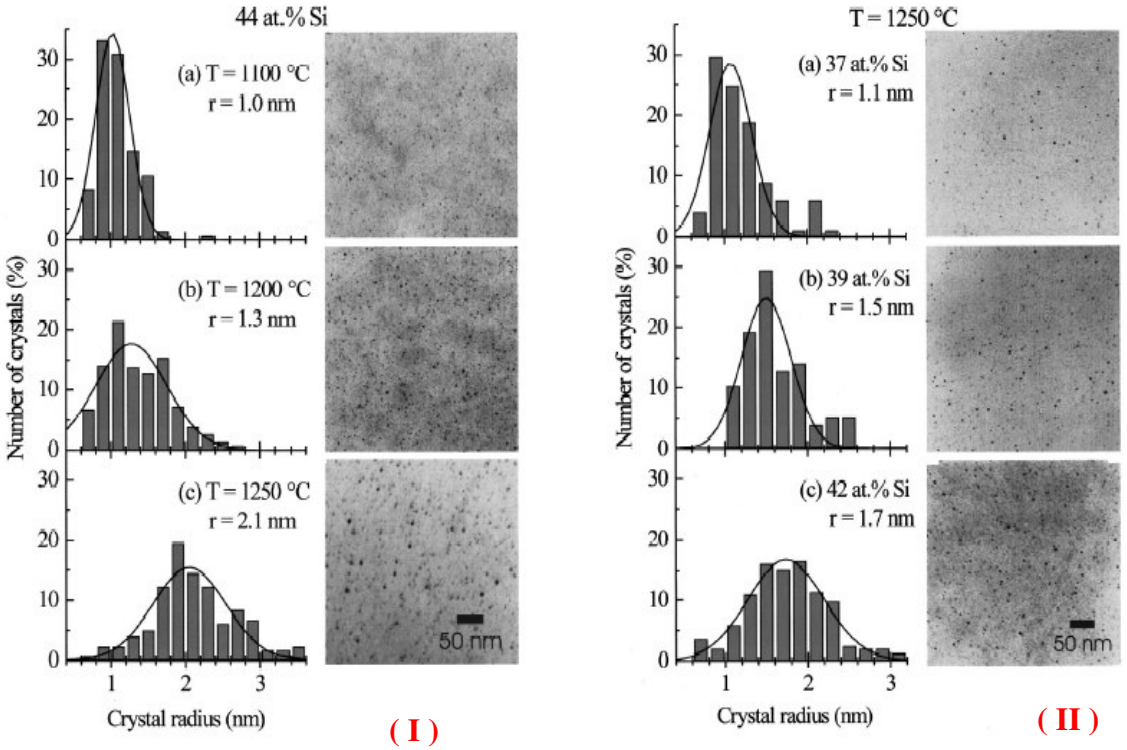

Fig.3.5.(I) Plan-view TEM micrographs and relative Si NC size distribution for a SiO*x* film having Si concentrations of 44 at. %, after annealing at a) 1100 °C, b) 1200 °C, and c) 1250 °C.**(II)** Plan-view TEM micrographs and relative Si NC size distribution for SiO*x* films having Si concentrations of a) 37 at. %, b) 39 at. %, and c) 42 at. %, after annealing at 1250 °C.

Fig 3.5 clearly shows the strong dependence of Si NC mean radius on both Annealing temperature and Silicon concentration, which in turn depends on inlet gas flow rate of PECVD.

4.1.Si NC formation:

We can schematically illustrate the heat-induced disproportionation reaction undergone by the intermediate $Si–Si_xO_{4-x}$ tetrahedra as

$$Si–Si_xO_{4-x} \rightarrow \frac{x}{4} Si–Si_4 + \left(1 - \frac{x}{4}\right) Si–O_4 \quad (x = 1,2,3)$$

The above reaction shows that the temperature-induced formation of SiO2 also involves the formation of a Si phase. Therefore, while as-deposited SiO_x films have the excess silicon atoms confined in partially oxidized tetrahedra (for low-temperature PECVD-deposited films only a very large silicon excess involves a relevant concentration of $Si–Si_4$ tetrahedra), in high-

temperature-annealed SiO_x films the excess silicon atoms are present as Si–Si4 tetrahedra, randomly dispersed in the amorphous SiO_2 matrix, and therefore, they have to be considered available for the nucleation and growth of silicon crystals.

4.2.Quantum Confinement Effect for PECVD grown Si NC:

The progressive blue shift of the PL peaks is observed in Figure 3.6 with decreasing the crystal size due to the enlargement of the band gap of the Si NC with respect to bulk crystalline silicon. This effect is dealt in more detail in chapter 4.

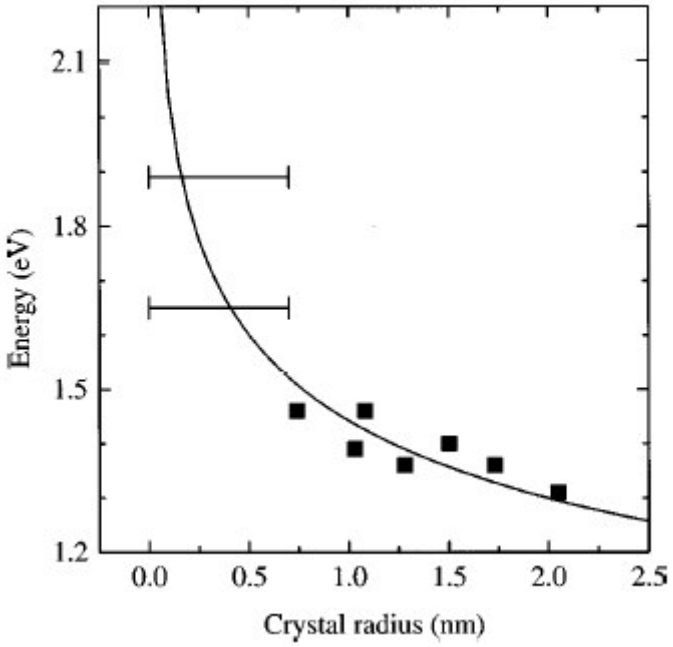

Fig 3.6 Energy of the luminescence peak vs Si NC mean radius, as obtained from TEM plan-view micrographs. The error bars refer to the PL peak of samples containing Si NC smaller than the TEM detection limit.

4.3. Quantitative analysis:

The energy needed for an atom to overcome the potential barrier is termed as the activation energy for surface diffusion. The average migration distance the Si atom migrates on the surface is given by[4],

$$\bar{x} = 1.4ae^{0.35\frac{Q_{des}}{kT}}$$

where a is the distance between adjacent lattice sites and Q_{des} is surface binding energy.

Aggregation of condensed species to form clusters of atoms possessing a specific volume(ie, bounded by a defined surface) is called nucleation. Nucleation rate can be determined by,

$$J = Kr^{*}a\sin\theta\frac{P}{\sqrt{2\pi mkT}}\exp\left[\frac{(Q_{des} - Q_{dif} - \Delta G^{*})}{kT}\right]$$

where

K = proportionality constant

r^{*} = critical radius (if the radius is larger than r^{*}, the particle is highly likely to be stable)

k = Boltzmann constant

T = Temperature in Kelvin

m = mass of the molecule

n_0 = Concentration of surface absorption sites available for nucleation

ΔG^{*} = Free energy of critical nucleus

P = System Pressure

The nucleation rate can be directly controlled by

1) The temperature
2) Critical nucleus radius
3) System Pressure
4) The angle of the cap, through surface cleanness

4.Quantum Mechanics Treatment of Nano Clusters

4.1 Quantum Confined Stark Effect:

Quantum confined stark effect (QCSE) is higly sensitive to the generation of electrons and holes. Electrons and holes screen the applied field and produce considerable changes in the optical spectra near the fundamental edge of absorption. These spectra become dependent on the concentration of the electron hole plasma, ie, on the intensity of light illumination. Moreover if the spectrum of the illuminating light is tuned into the region between exciton and interband absorption, QCSE produces bistable absorption, ie, for a given range of intensities of the incident light, both a high absorption state with large plasma concentration and a low absorption state with low plasma concentration can exist which is shown in fig 4.1[1].

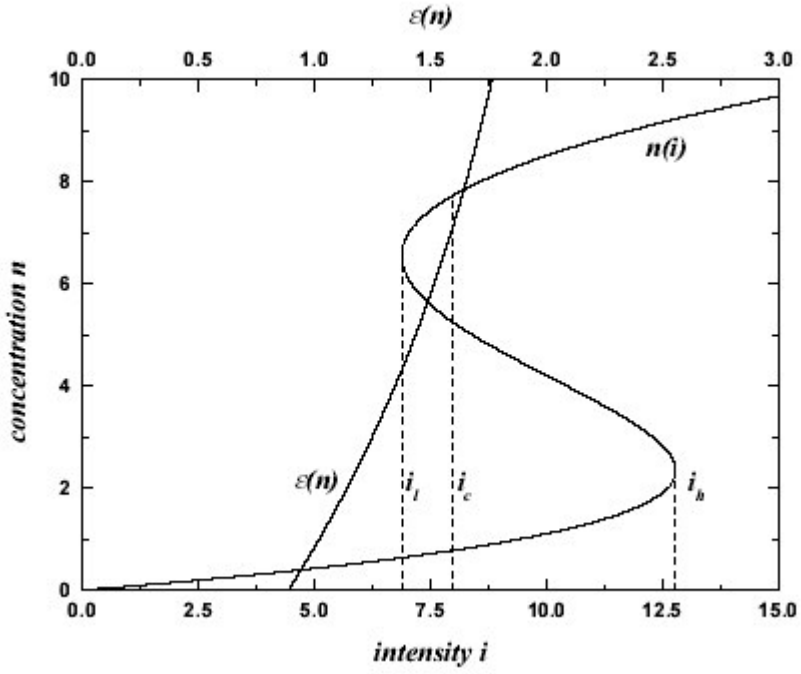

Fig.4.1. Renormalized energy å (scale on top of the figure) as a function of the plasma concentration *n* (left axis), and bistable characteristic curve n(i): plasma concentration as function of the incident light intensity *i* (left and bottom axis).

By Kramers- Kroing relation, when an electric field E is applied to the material, both the absorption and refractive index change,

$$\Delta n(\lambda) = 1 - \frac{\lambda^2}{2\pi^2} P \int_0^\infty \frac{\Delta\alpha(\lambda')}{\lambda'^2 - \lambda^2} d\lambda^2$$

$$\Delta\alpha(\lambda) = 8P \int_0^\infty \frac{\Delta n(\lambda')}{\lambda'^2 - \lambda^2} d\lambda^2$$ where P is the Principal value.

This describes the electro optic effect and a small applied voltage produces very large electric field, leading to a electroabsorption through QCSE, which can exceed 8000 cm^{-1}.

4.2.Quantum Confinement Effect:

Quantum confinement effect enhances the electron-hole radiative recombination rate[2]. When the cluster size is reduced below 10 nm, the electons and holes are confined as shown in fig 4.2 and their recombination results in emission of light.

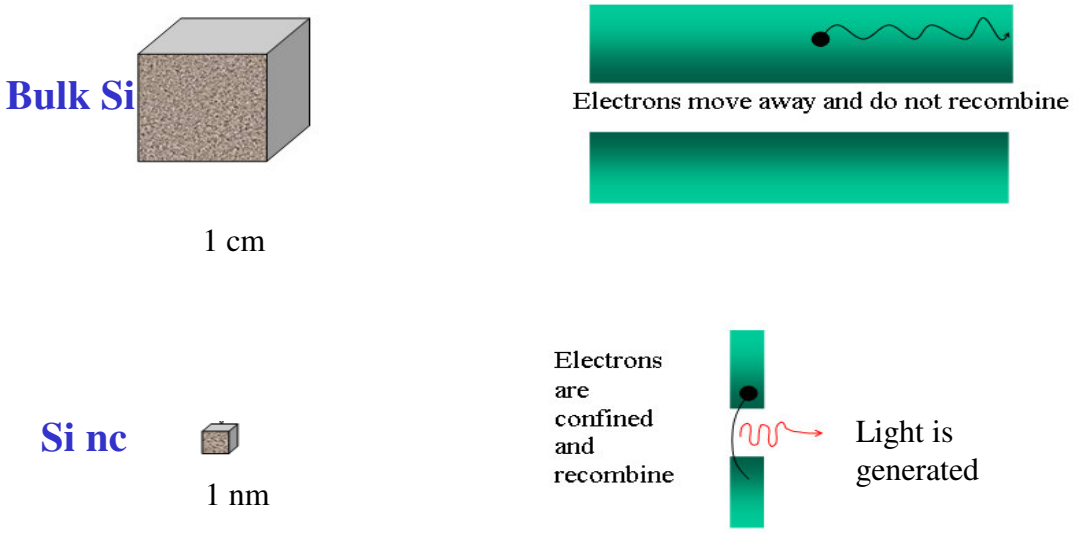

Fig.4.2 Quantum Confinement Effect

Figure 4.3 shows a sample of computed configurations for silicon clusters, respectively.It is interesting to note that Si clusters tend to form diamond-like, compact configurations[3].

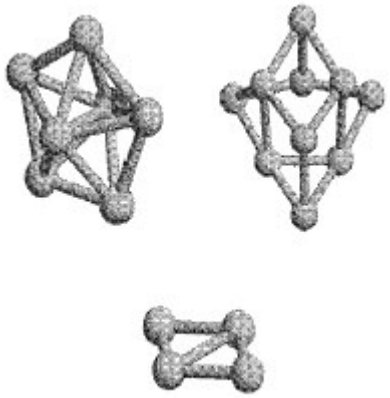

Fig 4.3 Possible configuration of Si NC

The quantum confinement effect changes the Bandgap of the material; For a-Silicon, bandgap is given as,

$$E(eV) = E_{bulk} + \frac{2.4}{a^2}$$

where E_{bulk} is the bulk *a*-Si band gap and a is the dot size.

Figure.4.4 shows the energy shift in the bandgap due to the quantum confinement effect.

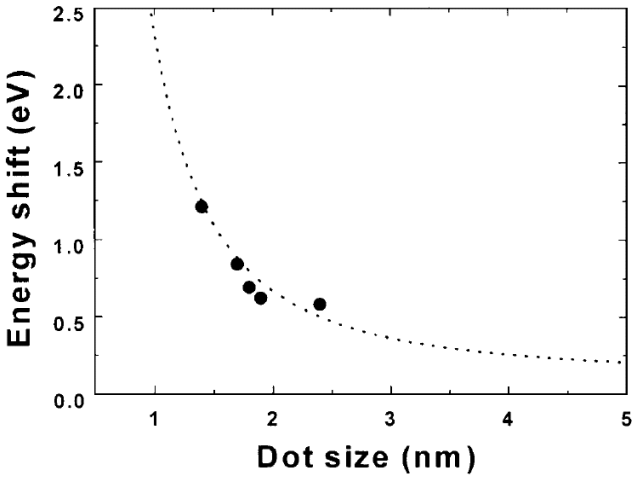

Fig.4.4 Energy shift Vs a-Si quantum dot size

The change in bandgap directly affects the radiative recombination rate, thus affecting the internal quantum efficiency of Si LED. The typical example is shown in fig 4.5.

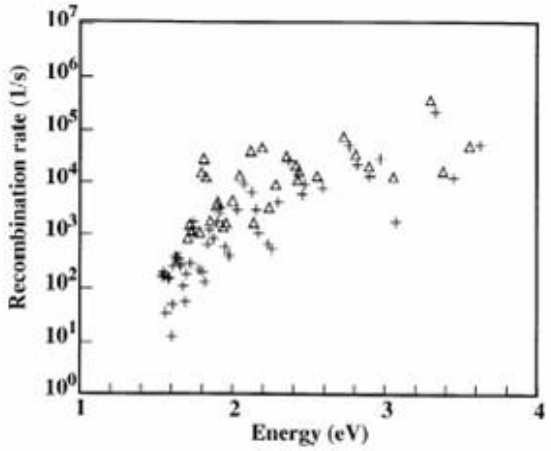

Fig.4.5 Radiative recombination rate calculated for clusters of $Si_{0.8}Ge_{0.2}$(triangles) and Si (crosses) with respect to their bandgap.

Quantum mechanically, there are three possible optical transitions in a nanocluster, namely a) Intraband transitions b) Interband transitions and c) the hot electron transitions. The intraband transitions originate in the filled conduction band states and terminate in other conduction band states which satisfy the selection rules for electric dipole transitions. Because both the initial and final states are free electron like, these transitions show the strongest quantum confinement effects, because the initial and final states both feel the effects of the boundary surface of the quantum dot. The interband transitions are from the d-like orbitals of the valence band to the empty conduction-band states. These states are only weakly dependent on quantum size effects because the initial state is already localized in space. Finally the hot electron transitions are those in which an electron in the conduction band absorbs a photon and is heated, losing its energy by electron photon scattering or collisions with the walls.

In the bulk semiconductor, the electron and hole are bound by the screened coulomb interaction with a binding energy of a few to tens of millielectron volts. The exciton is easily ionized at thermal energies, which accounts for the absence of a strong exciton absorption band

in a bulk semiconductor at room temperature. The exciton is a bound state of an electron and a hole by the coulomb interaction. By confining the electron and the hole in a nanoparticle, the binding energy and the oscillator strength can increase due to enhanced spatial overlap between the electron and the hole wave function and the coherent motion of the exciton. This confinement is responsible for the appearance of the exciton absorption in nanoparticles at room temperature. The exciton oscillator strength is given by

$$f = \frac{2m_e^*}{\hbar^2}\Delta E|M|^2\left|U_{(0)}\right|^2$$

where E is the transition energy, M is the transition dipole moment and is concerned with the probability of finding an electron and hole on the same site(the overlap). The oscillator strength per unit volume f/i (i being the cluster volume) determines the magnitude of the absorption coefficient. Thus absorption features of semiconductor nanoparticles are totally different from that of the bulk. For well sizes less than the Bohr radius of exciton, the excitons are confined in a quasi-two-dimensional potential, with the theoretical binding energy up to four times that of an unconfined exciton, which is otherwise less than thermal energy.

Many of the differences between the electronic behaviors of the bulk and the quantum confined low dimensional semiconductors are due to their difference in densities of states as shown in Figure 4.6.In case of zero dimensional systems such as nano clusters, the density of states is illustrated as the delta function. Optically, large absorption coefficients are observed.

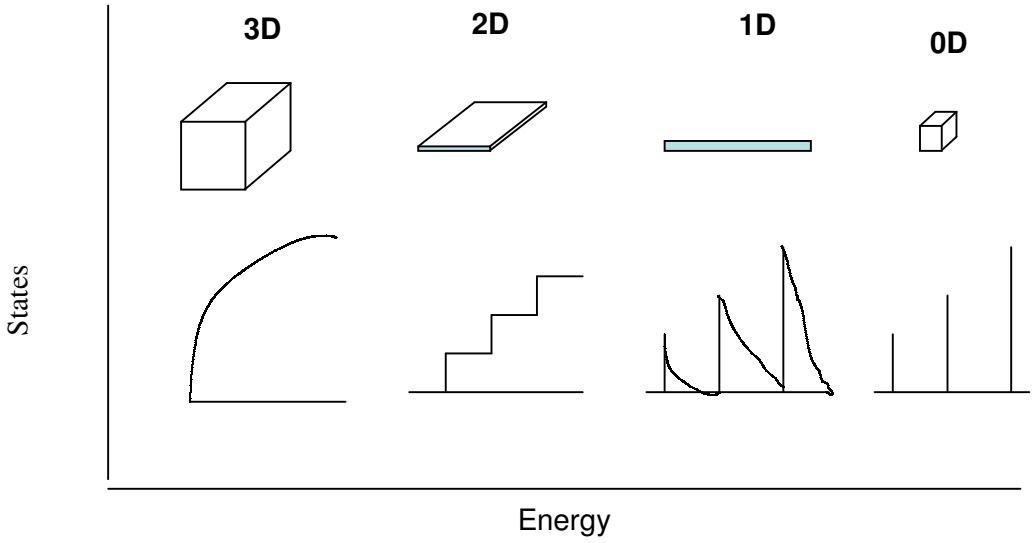

Fig.4.6 Variation in density of states of electrons with the increase of the quantization dimension in quantum structures.

The change in bandgap with respect to confinement factor can be found using many models. Their result is fit into figure 4.7[5].

Fig 4.7 Energy Gap Vs Confinement Factor 1/d

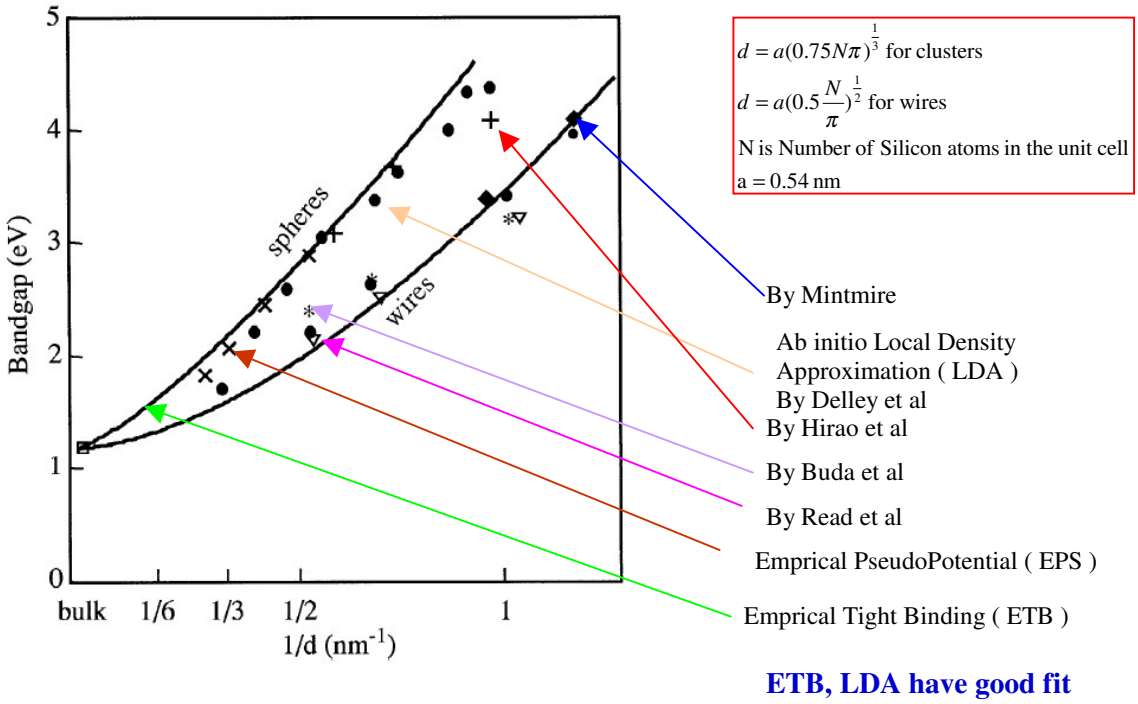

ETB, LDA have good fit

Reference

1.Introduction

1. Light emission from silicon : Progress towards Si-based Optoelectronics ; proceedings of Symposium B on Light Emission from Silicon : Progress towards Si-based Optoelectronics of the E-MRS 1998 Spring Conference ; Strasbourg, France, June 16-19, 1998 / edited by J. Linnros, F. Priolo, L. Canham.

2.Nanostructured Silicon

1. http://www.ece.rochester.edu/users/schan/sensor.html
2. Young-You Kim a, Jong-Hyun Jeon, Eun-Jun Ahn, Ki-WonLee, *Photoluminescence resonance properties of a porous silicon microcavity,* Sae Mulli Volume 44, Issue 4, 2002, Pages 224-228
3. http://www.ece.rochester.edu/users/schan/electrical.html
4. http://physics.ucsd.edu/~cciuti/optics.html
5. http://www.bath.ac.uk/physics/groups/opto/old/research.htm
6. http//www.ifm.liu.se/Matephys/AAnew/research/iii_v/easy0d1d.htm
7. http://www.bell-labs.com/project/oevlsi/tutorial
8. John Marsh, A primer on quantum well intermixing-catalyst technology for photonic integrated circuits, Intense Photonics

3.Plasma Enhanced Chemical Vapor Deposition of Silicon Nanocrystals

1. http://www2.eng.cam.ac.uk/~www-edm/equip.html#rfpecvd
2. Iacona, F., Franzo Á , G., and Spinella, C., 2000, *J. appl. Phys.*, **87,** 1295.
3. http://science.unitn.it/~semicon/

4. S.Sivaraman, Chemical Vapour Deposition, Thermal and Plasma Deposition of electronic materials,ITP Publishing Co.,1995.

Chapter 4:

1.L.L.Bonilla et al, Patterns under Quantum confined Stark Effect, J.Physics: Condensed Matter, 10 1998 L539

2. Nae-Man Park, Chel-Jong Choi, Tae-Yeon Seong, and Seong-Ju Park*,Quantum Confinement in Amorphous Silicon Quantum Dots Embedded in Silicon Nitride**,** *Department of Materials Science and Engineering and Center for Optoelectronic Materials Research, Kwangju Institute of Science and Technology, Kwangju, 500-712, Korea*

3. Gregory A. Johnson, Hierarchical modeling of C and Si nano-cluster nucleation utilizing quantum and statistical mechanics, Journal of Computer-Aided Materials Design 6(2): 337-347; Jan 1999

4. Handbook of Nanostructured Materials and Technology Vol 4 Optical Properties, edited by Hari singh Nalwa, Academic Press, 2000.

5. C.Delure,Optical band gap of Si nanoclusters, Journal of Luminescence,80 1999 65-73

5.Auger Recombination

1. Christoper John Williams, *Impact Ionisation and Auger Recombination in SiGe Heterostructures*,University of Newcastle.
2. A.Haug, *Auger recombination in quantum well semiconductors: calculation and with realistic energy bands*, Semicond. Sci. Tech. 7(1992)1337-1340.
3. Anatoli S.Polkovnikov and georgy G.Zegrya, Auger Recombination in semiconductor quantum wells, Ioffe Physico Technical Institute.
4. L. Dal Negro, M. Cazzanelli, Z. Gaburro, L. Pavesi,D. Pacifici, F. Priolo, G. Franzò and F. Iacona,*Optical gain in PECVD grown silicon nanocrystals*, SPIE Seattle2002 (To be published).

5. http://www.ioffe.rssi.ru/SVA/NSM/Auger/model.html